

# Controlling electron transfer processes through short molecular wires

E.G. Petrov<sup>a,\*</sup>, V. May<sup>b</sup>, P. Hänggi<sup>c</sup>

<sup>a</sup> Bogolyubov Institute for Theoretical Physics, National Academy of Sciences of Ukraine, Metrologichna str., 14-b, UA-03143, Kiev, Ukraine

<sup>b</sup> Institut für Physik, Humboldt Universität zu Berlin, Hausvogteiplatz, 5-7, D-10117, Berlin, Germany

<sup>c</sup> Institut für Physik, Universität Augsburg, D-86135, Augsburg, Germany

Received 2 November 2001

## Abstract

Current–voltage,  $I(V)$ , and current–magnetic field,  $I(h)$ , characteristics of a short molecular wire are studied in the framework of a model which accounts for strong Coulomb repulsion between the transferred electrons. The given approach avoids the fact that statistically the wire simultaneously transmits more than a single excess electron. First, we address short molecular wire systems which exhibit a narrow peak in the  $I(V)$ -characteristics. Recent experimental data of the peak current are well reproduced by our theory. In a second part, we study wires which contain paramagnetic ions mediating the ET. With the focus being on the low-temperature region, a step-like behavior of the current versus the magnetic field is predicted. © 2002 Elsevier Science B.V. All rights reserved.

**Keywords:** Electron transfer; Molecular wire; Magnetic field; Voltage bias; Coulomb repulsion; Paramagnetic ions; Nonlinear current

## 1. Introduction

Initiated by the suggestion of Aviram and Ratner [1] in the middle of the 1970s various schemes have been proposed where single molecules act as an active electronic device to achieve, for example rectification and gating of a current [2–8]. Meanwhile, the creation and characterization of such nano-scaled single-molecule systems

became possible of what can really be understood as the preliminary stage of *molecular electronics*. The archetype of all the discussed systems represents a linear-chain molecule which interconnects two micro-electrodes, thus forming a molecular wire. If a voltage is applied the transfer of electrons (or holes) can be controlled, and in this manner one can construct the current–voltage,  $I(V)$ , characteristics of a single molecule [9,10]. Once such a nano-structure has been formed, it becomes necessary to understand all the molecular properties which determine the  $I(V)$ -characteristics. But at the same time one is also faced with problems that relate to the molecule–electrode interaction.

\* Corresponding author.

E-mail addresses: [epetrov@bitp.kiev.ua](mailto:epetrov@bitp.kiev.ua) (E.G. Petrov), [may@physik.hu-berlin.de](mailto:may@physik.hu-berlin.de) (V. May), [hanggi@physik.uni-augsburg.de](mailto:hanggi@physik.uni-augsburg.de) (P. Hänggi).

The molecular properties mainly influence the manner the charge moves through the wire. This transport can take place either as an *elastic* electron transfer (ET) or as an *inelastic* transfer. If the Fermi levels of the two leads are arranged between the energetic positions of the HOMO and LUMO-levels of the wire and if the characteristic time of the hopping processes through the wire,  $\tau_{\text{hop}}$ , strongly exceeds the characteristic time of the direct wire-mediated tunneling,  $\tau_{\text{tun}}$ , the interelectrode current takes place as an elastic tunnel process. In such a situation the conductivity decreases exponentially with an increase of the wire length [9,11–13]. If the Fermi level is moved into resonance with the LUMO-levels the conductance oscillates with an increase of the wire [13,14]. Generally, the oscillations are caused by the dimensionality of the contacts and of the electrode, by the number of contacts, and by the microscopic geometry of the interface between the terminal part of the wire and the electrodes [15]. If, however,  $\tau_{\text{hop}} \ll \tau_{\text{tun}}$ , the current is determined by inelastic hopping transitions. Now, the electron tunneling is accompanied by energy dephasing at the terminal sites [16–20] as well as in the internal wire units [21–24].

In the case of elastic ET processes through the wire the corresponding theoretical models are more or less well established (see, e.g. [22]). Such a complete description does not exist in the case of hopping-like ET through the wire. This is in contrast to the description of ET reactions in donor-bridge-acceptor systems where the bridge may be given by a DNA fragment or a rigid oligopeptide. Indeed, a unified description of the elastic (superexchange) and inelastic (sequential) ET exist for the DNA [25,26] as well as the oligopeptide [27]. In particular, it could be demonstrated that the sequential ET mechanism becomes more efficient than the superexchange one if the number of bridging units is increased.

However, it is insufficient to remain at a description of single electron motion. In the presence of an electron reservoir given by the electrodes it becomes necessary to discuss the simultaneous motion of two or more excess electrons. Now, the current within the wire is strongly influenced by a Coulomb repulsion between the different and

simultaneously transferred electrons. Earlier theoretical studies carried out in the framework of a Hartree approximation indicate that even in the case of only two transferred electrons per wire the current-voltage characteristics strongly differs from that for a single transferred electron [28,29]. If the Coulomb electron-electron interaction is described within the Hubbard model a complicated nonlinear behavior of the wire mediated current is obtained [12,30].

Besides the important influence of the internal properties on the molecular wire conductivity the latter is also affected by the interaction of the terminal wire units with the micro-electrodes. The static part of this interaction can be sufficiently well described within the image force approximation [16,31,32]. It allows to estimate the polarization potential acting on the transferred electron and, in this manner, to specify the energy profile of the excess electron in the wire [23,33]. A microscopic description is achieved if quantum-chemical calculations are carried out on the molecule-metal interface [34,35]. Alternatively, a description has been proposed where the molecule and part of the surface atoms perturbed by molecular absorption define an “extended molecule” which in turn interacts with the rest part of the electrode [34,36].

Of course, the progress in the field of transport in a molecular wire strongly depends on a proper comparison of all ideas and theoretical concepts with experimental data, and in this manner the progress depends on the way to measure the current-voltage characteristics of different types of molecules and molecular complexes. First attempts to measure the current through a molecular wire date back to 1990 [37]. Meanwhile, nanofabrication techniques have been developed to contact single molecules [10,38], and starting from 1995 systematic measurements on the electron conduction through a single bridging molecule have been carried out [39–41].

The present paper presents results on the electron motion through molecular wires which are related to internal properties of the wire as well as to the wire-electrode interaction. We will describe *inelastic* ET, but with the restriction to short wires (less than 10 wire units). Upon extending recent quantum kinetic considerations and computations

on a nonlinear inelastic interelectrode current through a short molecular wire [23,24] we study in which manner the wire-mediated current can be controlled by steady electric and magnetic fields. The specificity of dealing with ET reactions through a short molecular wire lies in the very strong influence of the electrodes and the Coulomb repulsion (as in the case of ET through a single molecule [33,42]). Both disturbances, however,

become less prominent if the length of the wire is increased [23].

## 2. The basic theoretical model

For the following considerations we will employ a quantum kinetic ET model which has been recently proposed to study the inelastic interelectrode

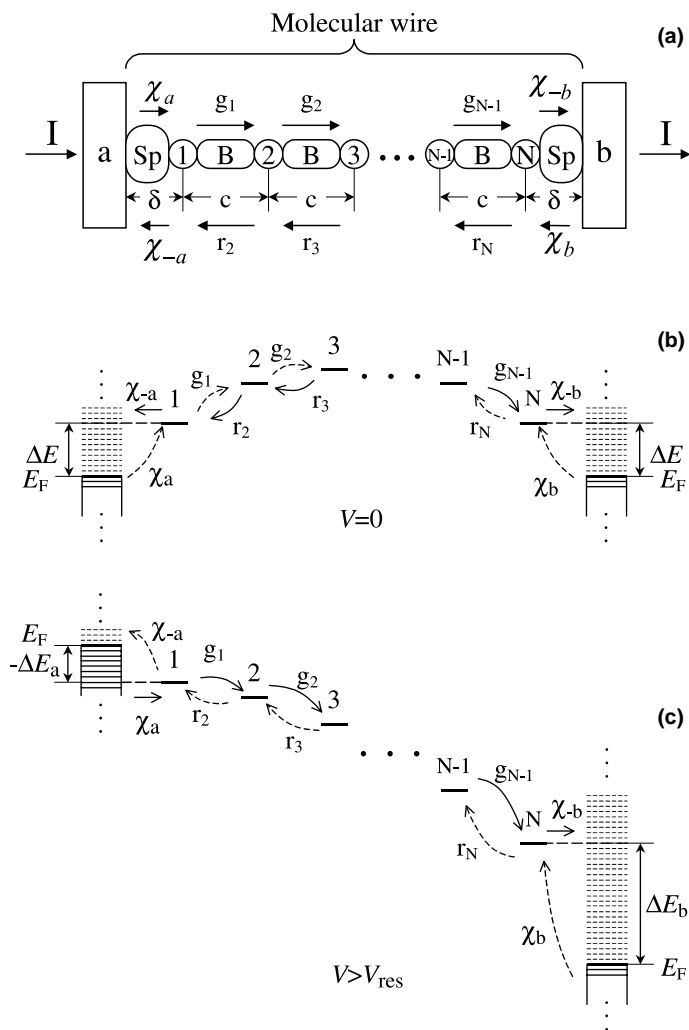


Fig. 1. Kinetic scheme of the ET through a linear molecular wire. Each terminal wire unit is connected with the corresponding electrode via the spacer (Sp) while the interior wire units are coupled by the bridging structures (B), see part (a). Due to the polarization shift caused by the electrodes all intersite transfer rates assume different values even at  $V = 0$ , see part (b). At a large voltage bias, the backward transfer rates become much smaller than the corresponding forward transfer rates, i.e.,  $r_{n+1} \ll g_n$ , part (c).

current through a short molecular wire [23,24]. The model is based on two main assumptions. First, the model assumes that the electronic coupling between the localization sites of the excess electron in the wire is weak compared to the electron–vibration interaction. This is typical for systems where the localization sites of the electron are separated by bridging ligands (e.g. oligoporphirin and polythiophene structures [6] or transition metal complexes [4], etc.). Accordingly, the ET through the molecular wire takes place as an electron hopping process characterized by rate expressions for the transition from electrode  $a$  ( $b$ ) to the wire ( $\chi_a$  and  $\chi_b$ ), for the reverse processes ( $\chi_{-a}$  and  $\chi_{-b}$ ), and for the wire-internal site to site transitions ( $g_n$ ,  $r_n$ , cf. Fig. 1(a)). The second assumption our model is based on, refers to the inter-electron Coulomb repulsion. It is supposed to be so strong in a short molecular wire that only a single electron can statistically be captured. Only if the excess electron already present in the wire leaves the wire can a new one enter. At room temperatures, such a blocking takes place if the wire length does not exceed 30–40 Å [23] (note that this estimate assumes a weak electronic intersite coupling which is unable to compensate the repulsion between the transferred electrons). As a result, ET through a short molecular wire proceeds as the motion of single electrons, but on the background of a strong Coulomb repulsion. If the wire does not contain paramagnetic ions and if no external magnetic field is present the following expression for the stationary interelectrode current (for any electron spin projection  $\sigma = \pm 1/2$ ) is valid [23,24]; i.e.

$$I = eW_0J. \quad (1)$$

Here,  $e$  is the elementary charge,  $J$  denotes the net electron flow through the wire, and

$$W_0 = \prod_{n=1}^N (1 - P_n)$$

gives the transmission factor taking notice of the strong Coulomb repulsion between the transferred electrons. The latter quantity can be expressed by the single-electron populations  $P_n$  of the wire units  $n = 1, 2, \dots, N$  (where  $N$  denotes the total number of localization sites in the wire). Consequently, a particular exclusion principle valid for short mo-

lecular wires results – the excess electron to be transferred through the wire can only enter it if any other excess electron already left the wire.<sup>1</sup>

For the following considerations it is advantageous to express  $W_0$  and  $J$  by the auxiliary quantities  $U_n \equiv P_n/(1 - P_n)$ , i.e.  $P_n = U_n/(1 + U_n)$

$$W_0 = \prod_{n=1}^N [1/(1 + U_n)], \quad (2)$$

and

$$J = \chi_a - \chi_{-a}U_1 = g_1U_1 - r_2U_2 = g_2U_2 - r_3U_3 \\ = \dots = \chi_{-b}U_N - \chi_b. \quad (3)$$

For any given number  $N$  of wire units the quantities  $U_n$  are derived from the system of equation (for further details see in [23]):

$$\sum_{m=1}^N A_{nm}U_m = C_n. \quad (4)$$

The elements of the transfer matrix  $\mathbf{A}$  are given by

$$A_{nm} = [(\chi_{-a} + g_1)\delta_{n,1} + (g_n + r_n)(1 - \delta_{n,1})(1 - \delta_{n,N}) \\ + (\chi_{-b} + r_N)\delta_{n,N}]\delta_{n,m} - g_{n-1}(1 - \delta_{n,1})\delta_{n,m+1} \\ - r_{n+1}(1 - \delta_{n,N})\delta_{n,m-1}, \quad (5)$$

while

$$C_n = \chi_a\delta_{n,1} + \chi_b\delta_{n,N}. \quad (6)$$

Noting Eq. (5) together with the relations (3) the net flow can be represented as

$$J = \frac{1}{\text{Det}(N)} (\chi_a g_1 \cdots g_{N-1} \chi_{-b} - \chi_b r_N \cdots r_3 r_2 \chi_{-a}), \quad (7)$$

where  $\text{Det}(N)$  denotes the determinant of the matrix  $\mathbf{A}$ . In the case of a wire with two or three sites the set ( $U_n$ ) are readily evaluated. For  $N = 2$  we obtain

$$U_1 = \frac{1}{\text{Det}(2)} [\chi_a \chi_{-b} + (\chi_a + \chi_b)r_2], \\ U_2 = \frac{1}{\text{Det}(2)} [\chi_{-a} \chi_b + (\chi_a + \chi_b)g_1] \quad (8)$$

<sup>1</sup> A similar exclusion principle has been already utilized to explain interference effects in resonance tunneling in coupled quantum wells [43].

and for  $N = 3$ , correspondingly,

$$\begin{aligned} U_1 &= \frac{1}{\text{Det}(3)} [\chi_a \chi_{-b} (g_2 + r_2) + (\chi_a + \chi_b) r_3 r_2], \\ U_2 &= \frac{1}{\text{Det}(3)} [\chi_a \chi_{-b} g_1 + \chi_{-a} \chi_b r_3 + (\chi_a + \chi_b) g_1 r_3], \\ U_3 &= \frac{1}{\text{Det}(3)} [\chi_{-a} \chi_b (g_2 + r_2) + (\chi_a + \chi_b) g_1 g_2]. \end{aligned} \quad (9)$$

The corresponding determinants read

$$\begin{aligned} \text{Det}(2) &= \chi_{-a} \chi_{-b} + \chi_{-a} r_2 + \chi_{-b} g_1, \\ \text{Det}(3) &= \chi_{-a} \chi_{-b} (g_2 + r_2) + \chi_{-a} r_3 r_2 + \chi_{-b} g_1 g_2. \end{aligned} \quad (10)$$

Eqs. (1), (2), and (7) enable one to evaluate the interelectrode current in those short molecular wires where the current results from a hopping mechanism of ET. The specifics of the electrode–molecular wire–electrode nano-structure is given by the single-electron transfer rates  $g_n$ ,  $r_n$ ,  $\chi_a$ ,  $\chi_{-a}$ , and  $\chi_b$ ,  $\chi_{-b}$ . Just such types of short molecular wires are expected to be the best candidates for an experimental observation of inelastic currents. If magnetic interactions are important the spin-state dependence of the rates have to be taken into account, cf. the examples in [17,18]. We will discuss this question in Section 4 of this paper.

### 3. Nonlinear properties of an interelectrode current

It has been already demonstrated before in [23] that the current–voltage characteristics of the electrode–molecular wire–electrode nano-structure become nonlinear if the Coulomb repulsion between the transferred electrons is accounted for. First, there is a rising of the current with increasing voltage towards a saturation. Second, an abrupt decrease of the current appears if the voltage is increased further. This nonlinear behavior follows from the electrode wire model including the averaged polarization. In particular, it becomes possible to present an analytical expression for the current which is valid at any voltage bias. In this model the abrupt decrease of the current is originated by the decrease of the transmission factor  $W_0$ , see Eq. (2). The following considerations are

devoted to a detailed inspection of this important blocking phenomenon.

#### 3.1. Interelectrode current at large voltages

To determine the interelectrode current the basic Eqs. (1), (2), and (7) have to be specified by concrete expressions for the transfer rates. We restrict ourselves to the consideration of a regular wire and use the same rate expressions as in [23]; i.e. the Jortner form of the ET-transfer rates [44]. The intersite transfer rates read

$$\begin{aligned} r_{n+1} &= \exp[-(E_n - E_{n+1})/k_B T] g_n, \quad g_n = \alpha_0 \Phi_{v_n}, \\ \Phi_{v_n} &= \exp[-S \coth \hbar \omega_0 / 2k_B T] \\ &\quad \times \{ [1 + n_B(\omega_0)] / n_B(\omega_0) \}^{v_n/2} \\ &\quad \times I_{|v_n|} \left( 2S \sqrt{n_B(\omega_0)(1 + n_B(\omega_0))} \right). \end{aligned} \quad (11)$$

The electrode–wire and wire–electrode transfer rates (for electrode a) have the form

$$\chi_a = \exp[-\Delta E_a / k_B T] \chi_{-a},$$

and

$$\chi_{-a} = \chi_0 [1 - n_F(\Delta E_a)] \Phi_0, \quad (12)$$

respectively. Both expressions are valid in a similar form for  $b$  replacing  $a$ . In Eq. (11) we introduced the Bose distribution  $n_B(\omega_0) = [\exp(\hbar \omega_0 / k_B T) - 1]^{-1}$  while in Eq. (12),  $n_F(\Delta E_{a(b)}) = [\exp(\Delta E_{a(b)} / k_B T) + 1]^{-1}$  is the Fermi distribution functions. Furthermore,  $\omega_0$  denotes the frequency of an active vibrational mode strongly coupled to a heat bath, we introduce  $\Delta E_a = E_1 - E_F - eV$ ,  $\Delta E_b = E_N - E_F$  where  $V$  is the applied voltage bias,  $E_F$  is the Fermi-level energy, we set  $S \equiv \lambda / \hbar \omega_0$  ( $\lambda$  is the reorganization energy), and  $I_\nu(z)$  gives the modified Bessel function. The voltage and temperature independent constants introduced in Eqs. (11) and (12) are given as

$$\alpha_0 = 2\pi |V_{s-s}|^2 / \hbar^2 \omega_0, \quad \chi_0 = (2\pi |V_{s-e}|^2 / \hbar E_F) C, \quad (13)$$

where  $V_{s-s}$  and  $V_{s-e}$  are electron couplings between neighboring wire sites and between the terminal sites of the wire and the nearest surface metal atom, respectively. The newly introduced factor  $C$  accounts for the properties of the electrode metal

surface as well as the structure of the terminal wire unit. To specify this factor it becomes necessary to perform detailed quantum-chemical calculations. A simple estimate is possible in the framework of the electron gas model and for a cubic metal. It yields  $C \approx (a_c k_F)^3 / 4\pi$  where  $a_c$  is the crystallographic cell constant and  $k_F$  denotes the Fermi vector. Assuming  $E_F \sim 5$  eV and thus  $k_F \sim 10^8$  cm/s, one obtains  $C \sim 1$ .

Of particular importance for the ET reaction are the parameters

$$v_n \equiv (E_n - E_{n+1}) / \hbar\omega_0 \quad (14)$$

which define (in units  $\hbar\omega_0$ ) an energy bias between the electronic localization sites. If  $v_n > 0$  the backward site to site transfer rates  $r_{n+1}$  become smaller than the corresponding forward transfer rates  $g_n$ . The electrostatic potential along the wire assumes with  $v_n > 0$  the form

$$E_n = E_0 + eV(1 - x_n/L) + E^{(i)}(x_n). \quad (15)$$

This expression shows that the site energy of the transferred electron (at wire unit  $n$ ) is the sum of unperturbed LUMO-level energy, i.e.,  $E_0$ , the linear ramp, and the polarization shift

$$E^{(i)}(x_n) = -\frac{13.5}{\varepsilon} \left\{ \frac{K}{2} \left( \frac{1}{x_n} + \frac{1}{L-x_n} \right) + \frac{1}{2} \sum_{m=1}^{\infty} K^{2m} \right. \\ \left. \times \left[ K \left( \frac{1}{Lm+x_n} + \frac{1}{L(m+1)-x_n} \right) - \frac{2}{Lm} \right] \right\}. \quad (16)$$

This expression follows from a general form of the image-force potential originated by metallic plates [16,45]. Note, that  $E^{(i)}(x_n)$  is given in eV, while the total length of the wire  $L = 2\delta + (N-1)c$  and the positions of electron localization  $x_n = \delta + (n-1)c$  (cf. Fig. 1(a)) are taken in Å. In Eq. (16) we introduced  $K \equiv (\varepsilon_e - \varepsilon) / (\varepsilon_e + \varepsilon)$  with  $\varepsilon_e$  and  $\varepsilon$  as the electrode and interelectrode medium permittivities, respectively. Eq. (16) defines a complicated non-monotonic potential profile for the transferred electron within the wire. However, for a large applied voltage the linear ramp can compensate the decrease of energy caused by the electrodes (Fig. 2) so that the property  $v_n > 0$  is satisfied for all wire units. Now, the forward rates substantially exceed

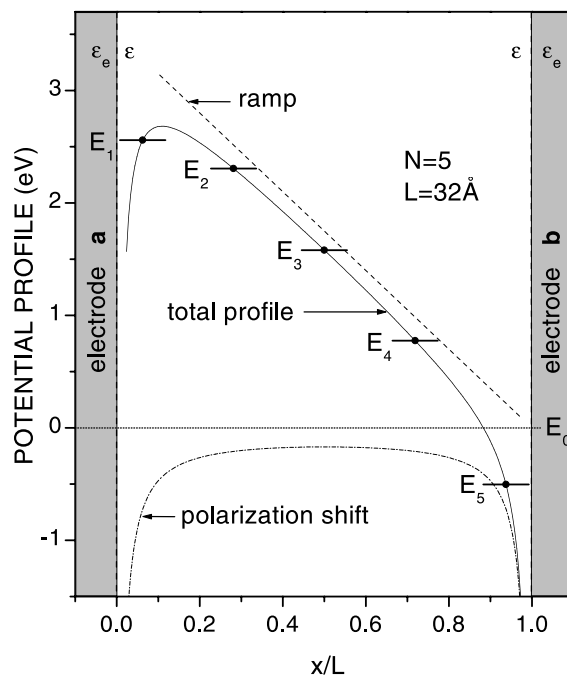


Fig. 2. Formation of the overall potential profile for the transferred electron. The position of the electron is given via the dimensionless distance  $x/L$ . The electronic energies  $E_n$  are arranged relative to the unperturbed LUMO-level  $E_0$ . Calculations have been done in using Eqs. (15) and (16),  $E_0 = 0$ ,  $\varepsilon = 4$  and  $\varepsilon_e = 1000$ .

the corresponding backward rates. Fig. 1(c) illustrates such a situation indicating the small transfer rates by dashed arrows. Consequently, a large voltage bias  $V$  leads to an unidirectional left-to-right ET through the wire.

Fig. 3 nicely depicts that the increase of the current generally results from the increase of the flow. However, the decrease of the current which takes place if  $V$  is further increased, completely results from that of the transmission factor  $W_0$ . Comparing Fig. 3(a) with Fig. 3(b) one notices the large difference with respect to the magnitude of the flow saturation as well as with respect to the peak (plateau) of the current. The behavior shown in Figs. 3(a) and (b) is originated by a large difference with respect to the reorganization energy  $\lambda$  (or by the dimensionless parameters  $S = \lambda / \hbar\omega_0$  with fixed vibrational frequency  $\omega_0$ ). This different behavior can be explained in noting that the peak (plateau) of the current appears if a resonant

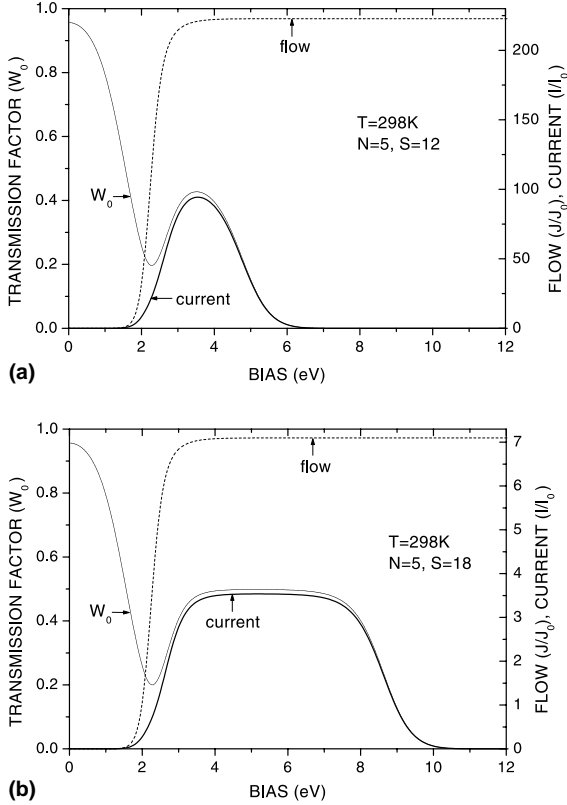


Fig. 3. Formation of the current through a wire with five units. The current and the flow are measured in units of  $I_0 \equiv 10^{-6} I_s$  ( $I_s \equiv e\chi_0$ ) and  $J_0 \equiv 10^{-6} J_0$ , respectively. The rise of the current is caused by the rise of the flow while the transmission factor is ruling the current decrease. The maximal value of the current corresponds either to the peak value, part (a) or to the plateau, part (b). Calculations have been done based on Eqs. (1), (2), (4), (5), (6), (7), (11) and (12). The remaining parameters are  $\Delta E_0 \equiv E_0 - E_F = 0.82$  eV,  $\omega_0 = 500$   $\text{cm}^{-1}$ ,  $\varepsilon = 4$ ,  $\varepsilon_e = 1000$ ,  $\zeta = 0.3$ ,  $\delta = 2$  Å,  $c = 7$  Å,  $L = 32$  Å.

tunneling from the left electrode to the corresponding terminal wire unit is switched on [23]. This resonant ET occurs at voltages where  $\Delta E_a \equiv e(\delta/L)(V_{\text{res}} - V) \leq 0$ . Here, we used

$$V_{\text{res}} = \Delta EL/e\delta \quad (17)$$

and  $\Delta E \equiv E_0 - E_F + E^{(i)}(x_1)$  (cf. Fig. 1(b)). We can therefore conclude that for  $\exp(\Delta E_a/k_B T) \ll 1$  and  $\exp[-(E_n - E_{n+1})/k_B T] \ll 1$  with  $V > V_{\text{res}}$  the following inequalities for the electrode–wire and wire–electrode transfer rates result; i.e.  $\chi_a \gg \chi_{-a}$ ,  $\chi_{-b} \gg \chi_b$  as well as for the wire-internal rate con-

stants,  $g_n \gg r_{n+1}$ , respectively. These inequalities indicate that one can utilize at large  $V$  the approximation of vanishing backflow, i.e.,

$$\chi_{-a} = r_2 = r_3 = \dots = r_N = \chi_b = 0. \quad (18)$$

Noting the relations (3) we next derive the simplified, large voltage expressions

$$U_N \simeq \chi_a/\chi_{-b}, \quad U_n \simeq \chi_a/g_n \quad (n = 1, 2, \dots, N-1), \quad (19)$$

while

$$J \simeq \chi_a, \quad W_0 \simeq \left( \frac{1}{1 + \chi_a/\chi_{-b}} \right) \prod_{n=1}^{N-1} \left( \frac{1}{1 + \chi_a/g_n} \right). \quad (20)$$

It is not difficult to determine the dependency of the current on the applied voltage within these approximations. Let the vibration energy  $\hbar\omega_0$  exceed the thermal energy  $k_B T$  so that  $n_B(\hbar\omega_0) \ll 1$ . In this case – and if  $S$  is not too large – the argument of Bessel function appearing in Eq. (11) reduces to a small value and thus the asymptotic form  $I_\nu(z) \approx (z/2)^\nu/\Gamma(\nu+1)$  [46], with  $\Gamma(x)$  the Gamma-function, becomes valid independently of the particular value of  $\nu$ . Correspondingly, Eq. (11) reduces to the expression [47]

$$\Phi_{\nu_n} \approx e^{-S} S^{\nu_n} / \Gamma(\nu_n + 1), \quad (21)$$

with  $\nu_n$  given in Eq. (14). It follows from Eqs. (12), (20) and (21) that the flow  $J$  possess a maximum,  $J_{\text{max}} = \chi_0 \exp(-S)$ . Therefore, if  $\chi_0$  is fixed, the flow increases if  $S$  decreases, cf. Figs. 3(a) and (b).

To analyze the abrupt decrease of the current in more detail we note that the quantity

$$\chi_a/g_n = (\Gamma(\nu_n + 1)/S^{\nu_n}) \zeta^{-1} n_F(\Delta E_a), \quad (22)$$

with  $\zeta \equiv \alpha_0/\chi_0$ ,

which specifies the transmission factor  $W_0$ , cf. Eq. (20), strongly increases with increasing value  $\nu_n$ . Actually, at large  $V$  when  $\nu_n \gg 1$  we can take the asymptotic expansion  $\Gamma(\nu+1) \approx \sqrt{2\pi/\nu} \nu^\nu \exp(-\nu)$  which allows us to reduce Eq. (22) to the simpler form

$$\chi_a/g_n = \zeta^{-1} \sqrt{2\pi/\nu_n} \exp(-\nu_n) \exp[\nu_n(\ln \nu_n - \ln S)]. \quad (23)$$

In passing we remark that we also used the fact that for  $V > V_{\text{res}}$  one can set  $n_{\text{F}}(\Delta E_a) \approx 1$ . It can be recognized that a sudden drop of  $\chi_a/g_n$  occurs if  $v_n > S$ . Let us take into consideration that  $v_n$  gives the mean number of vibrations accompanying the jump of the transferred electron from the  $n$ th to the  $(n+1)$ th wire unit, cf. definition Eq. (14). If more quanta are involved the jump efficiency becomes less efficient. For large  $V$ ,  $v_n$  is also large and thus the forward transfer rate  $g_n$  is small. This fact indicates that the limiting step of the ET through the wire are the hops between the wire units. As a result, the transferred electron is slowed down within the wire, the site populations  $P_n$  increase and thus the transmission factor becomes drastically reduced. Hence, the current is blocked. The inequality  $v_n > S$  is identical to  $E_n - E_{n+1} > \lambda$ , which states that the decrease of the current with the rise of the  $V$  occurs if the driving force of the site to site ET process induced by the applied electric field starts to exceed the corresponding reorganization energy.

### 3.2. Current through a wire with two electronic localization sites

According to Eqs. (20) and (23) a control of the interelectrode current eq. (1) can be achieved by an alteration of the parameters  $\zeta$  and  $S$ . Increasing any of these parameters the formation of the plateau becomes easier, see [23] where the influence of the parameter  $\zeta$  has been discussed, and also in Figs. 3(a) and (b) with curves valid for different  $S$ . A large value of  $v_n$  and, thus, of the driving force for the site to site transitions is reached if a wire with a large distance between neighboring sites is taken. Now, the blocking of the current might be observed at a smaller voltage compared to the case of a wire with more units. Fig. 4 depicts the form of the nonlinear current through a wire with *two sites*. The calculations are carried out by use of Eq. (1) with the form of the flow  $J$  given by

$$J = \frac{\chi_a \chi_{-b} g_1 - \chi_{-a} \chi_b r_2}{\chi_{-a} \chi_{-b} + \chi_{-a} r_2 + \chi_{-b} g_1} \quad (24)$$

and the transmission factor reads

$$W_0 = [(1 + U_1)(1 + U_2)]^{-1}. \quad (25)$$

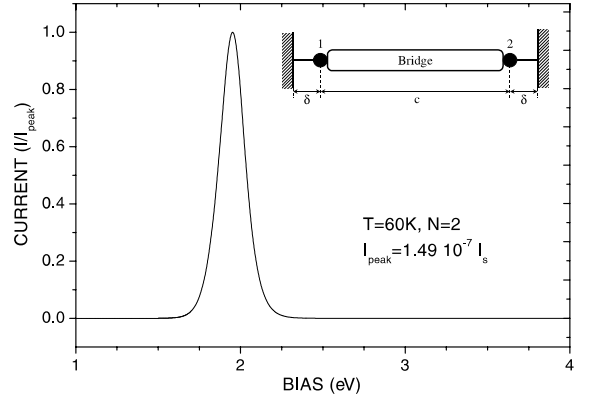


Fig. 4. Formation of the peak current through a wire with two sites of electron localization for the transferred electrons. The peak current is expressed via the quantity  $I_s \equiv e\chi_0$ . Calculations have been done based on Eqs. (24) and (25) and in taking  $\varepsilon = 4$ ,  $\varepsilon_e = 1000$ ,  $T = 60$  K when  $\delta = 3.2$  Å,  $c = 16.7$  Å,  $\zeta = 0.5$ ,  $S = 12$ ,  $\omega_0 = 355$  cm $^{-1}$ ,  $\Delta E_0 = 0.76$  eV.

Here,  $U_1$  and  $U_2$  are given by Eqs. (8) and (10). The expressions for  $J$  and  $U_n$  can be simplified if one notes that for  $V \geq V_{\text{res}}$  the rates  $\chi_b$  and  $r_2$  assume very small values. By use of the condition  $\chi_b \approx 0$ ,  $r_2 \approx 0$  it follows that

$$J = \chi_a \frac{g_1}{g_1 + \chi_{-a}}, \quad U_1 = \frac{\chi_a}{g_1 + \chi_{-a}}, \quad (26)$$

$$U_2 = \left( \frac{\chi_a}{\chi_{-b}} \right) \frac{g_1}{g_1 + \chi_{-a}}.$$

According to the expression of  $J$  we may conclude that in the resonance region  $V > V_{\text{res}}$  the flow can assume a plateau (it occurs if  $g_1 \gg \chi_{-a}$  and thus  $J \approx \chi_a \approx \chi_0 \exp(-S)$ ), followed by an decrease which is originated by the sudden drop of the forward site to site transfer rate  $g_1$  (it occurs when  $g_1 \ll \chi_{-a}$  and thus  $J \approx (\chi_a/\chi_{-a})g_1$ ). The simplified expression (26) is sufficient for an evaluation of the current in the vicinity of its maximum as well as for  $V > V_{\text{res}}$ . It follows from Eqs. (1) and (26) that in the case when the flow has a plateau, i.e., at  $g_1 \gg \chi_{-a}$ , the current emerges as

$$I = e\chi_a \left( \frac{1}{1 + \chi_a/g_1} \right) \left( \frac{1}{1 + \chi_a/\chi_{-b}} \right)$$

$$\approx \begin{cases} \frac{eg_1}{1 + \chi_a/\chi_{-b}} & \text{if } \chi_a \gg g_1, \\ \frac{e\chi_a}{1 + \chi_a/\chi_{-b}} & \text{if } g_1 \gg \chi_a. \end{cases} \quad (27)$$

Eq. (27) refers to the case when only a one-way ET is realized through the wire.

Fig. 4 depicts the  $I(V)$ -characteristics for two identical electrodes and a wire with two identical units. In contrast to the case of a five-units wire, cf. Fig. 3(a), we can choose the set of parameters if the current peak is reached at  $V = 2$  eV (the corresponding value for  $N = 5$  is  $V = 4$  eV). Besides, for  $N = 2$  the width became much more smaller compared to  $N = 5$ . In Fig. 4, the localization sites of the transferred electron correspond to the position of the terminal atoms contacting the electrode surface (e.g. sulfur or carbon atoms, see the discussion in [36,41,42]) while the remaining part of wire modulates the bridging system. Note that our theory predicts a rather narrow peak in the  $I(V)$ -characteristics. A similar narrow peak has been observed in experiments using a nanopore system doped with molecules which are responsible for a nonvanishing conduction of the nanopore [40].

#### 4. Low temperature current in presence of a magnetic field

In this section we study inelastic ET reactions through a short molecular wire for the case where the wire units contain paramagnetic ions. For an example of such units we refer to metalloporphyrin molecules and metal–ligand compounds [4,48]. In such a case, the specific properties of the paramagnetic ions can come into play if a low temperature region is chosen where the Zeeman splitting of the spin levels in the magnetic field is comparable to the thermal energy  $k_B T$ . In [17,18], the particular case has been studied where two nonmagnetic electron localization sites in the wire are connected by a bridging system and just this system contains one or two coupled paramagnetic ions.

Here, we consider the somewhat different situation of a wire with two sites each with a paramagnetic ion. Ligands surrounding the ions create a crystal field which is responsible for the formation of a definite electronic configuration for each ion. The ions are separated by a nonmagnetic bridging system. We restrict ourselves to the case

where each paramagnetic ion has a “frozen” angular momentum in the ground state so that the ion spin  $S$  and its projection  $M$  represent good quantum number. Additionally, it will be assumed that each ion has a number of electrons in its incompletely filled shell equal to or larger than the number of one-electron states in this shell. As an example, we refer to the ions  $\text{Mn}^{2+}$ ,  $\text{Fe}^{3+}$ , and  $\text{Ni}^{2+}$ . The first two ions possess an electronic configuration (in the cubic field)  $t_{2g}^3 e_g^2$  with the ion spin  $S = 5/2$  while the electronic configuration of  $\text{Ni}^{2+}$  is  $t_{2g}^6 e_g^2$  with  $S = 1$ . The addition of a single electron changes the above-mentioned configurations into  $t_{2g}^4 e_g^2$  and  $t_{2g}^6 e_g^3$ , respectively. The corresponding spins become equal to  $S' = 2$  and  $S' = 1/2$  [48].

Let us consider the formation of a current at  $V > V_{\text{res}}$  and at low temperatures. In this case the conditions in Eq. (18) are satisfied in an excellent manner and, correspondingly, only one-way ET proceeds through the wire. Furthermore, we assume that rate for the electrode–site transitions  $\chi_a$  and  $\chi_{-b}$  strongly exceed the forward site to site rate  $g_1$  and, additionally,  $\chi_{-b} \gg \chi_a$ . Such an inequality can become valid even for the case of identical wire units where, e.g. the left and the right spacers, Sp1 and Sp2, have a different atomic structure, cf. insertion in Fig. 5. Bearing in mind the above-given inequalities and utilizing Eq. (27) one derives  $I_{+1/2} = I_{-1/2} = I = eg_1$  where  $I_\sigma$  is the partial component of the current corresponding any spin-projection  $\sigma$  of the transferred electron.

If a magnetic field  $\mathbf{h}$  is applied, a discrimination between the two components  $I_{+1/2}$  and  $I_{-1/2}$  takes place and thus  $I_\sigma = eg_{1\sigma}$ . To derive an expression for the total current  $I_{\text{tot}} = \sum_\sigma I_\sigma$  we have to note that the characteristic value of the magnetic energy,  $\mu_B gh$  ( $\mu_B$  and  $g$  are the Bohr magneton and  $g$ -factor, respectively), is very small compared to the Fermi-level  $E_F$ . Hence, the inequality  $\mu_B gh \ll E_F$  indicates that an applied magnetic field has a negligible effect on the electrons in the electrodes [49]. We thus can ignore this magnetic energy. Below we will utilize such a model for an electron–vibration coupling which results in an expression for the forward site to site transition rate similar to that of Eq. (11). The magnetic energy  $\mu_B gh$  is assumed to be small compared with the characteristic vibrational energy  $\hbar\omega_0$ . As a result the

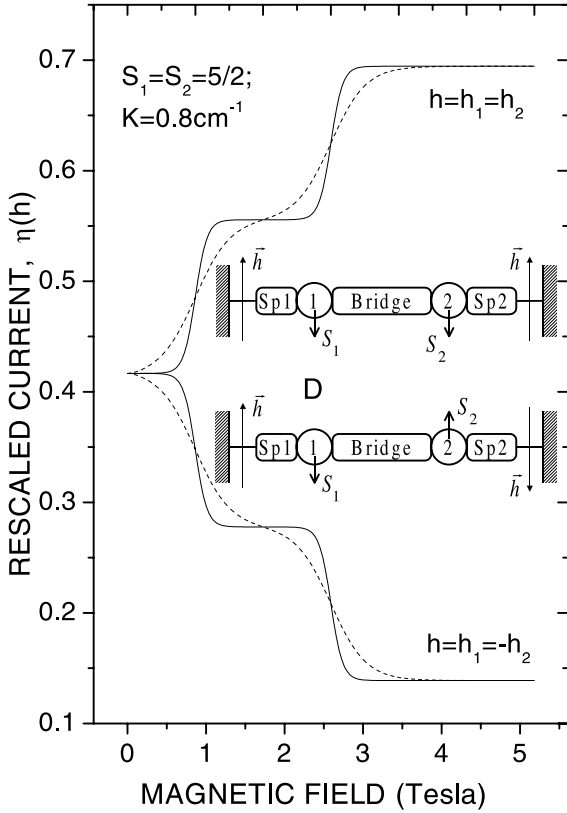


Fig. 5. Step-like formation of a low-temperature interelectrode current mediated by the wire of two units. The units contain identical paramagnetic ions with frozen angular momenta and with spins  $S_1 = S_2 = S$ . The quantization axis  $z$  is directed along the magnetic field  $\mathbf{h} = \mathbf{h}_1$ , and the magnetic field  $\mathbf{h}_2$  is oriented either parallel to  $\mathbf{h}_1$  or antiparallel. Calculations have been done based on Eqs. (31)–(33) and with  $S = 5/2$ ,  $g = 2$ ,  $K = 10^{-4}$  eV; solid and dashed line correspond to the temperatures  $T = 10^{-5}$  and  $T = 3 \times 10^{-5}$  eV, respectively.

magnetic field dependence of the factor  $\Phi_v$  can safely be neglected.

For the following we will assume that the molecular wire consists of two identical units with identical paramagnetic ions. Furthermore, we set  $S_1 = S_2 = S$  for the spin values of the ions, and provide that the transferred electron can be captured by the paramagnetic ions in the course of the ET through the wire. And finally we suppose that the electronic coupling between the sites occurs via the superexchange mechanism. In this case, the spin dependence of the site to site coupling  $V_{s-s}$ , which specifies the parameter  $\alpha_0$ , Eq. (13), is given

by the well-known expression  $V_{s-s} = V_{b_N}^* G_{b_N b_1} V_{1 b_1}$ , see e.g. [11,49]. Here  $G_{b_N b_1}$  is the Green function of the bridge of  $N$  units while  $V_{1 b_1}$  ( $V_{2 b_N}$ ) denotes the coupling between the first (second) paramagnetic ion and the adjacent  $b_1$ th ( $b_N$ )th bridge unit. The bridge should be a nonmagnetic system and thus only the couplings  $V_{1 b_1}$  and  $V_{2 b_N}$  depend on the spin states of the paramagnetic ions. Noting that the considered paramagnetic ions reduce their spin from  $S$  to  $S - 1/2$  if an extra electron is captured we can take the expressions for the matrix elements  $V_{1 b_1}$  and  $V_{2 b_N}$  given in [18]. Denoting the spin projection of the reduced ion by  $M'_{1(2)}$  (where  $-(S - 1/2) \leq M'_{1(2)} \leq (S - 1/2)$ ) and the spin projection of the nonreduced ion via  $M_{1(2)}$  (where  $-S \leq M_{1(2)} \leq S$ ) one derives

$$V_{s-s} = V_{s-s}^0 F(\sigma; M_1, M_2; M'_1, M'_2). \quad (28)$$

Here,  $V_{s-s}^0$  is the reduced matrix element which is independent on the spin-projection of the electron and the ions. This dependence is contained in the factor

$$F(\sigma; M_1, M_2; M'_1, M'_2) = C_{(1/2)\sigma SM_2}^{(S-1/2)M'_2} \times C_{(1/2)\sigma SM_1}^{(S-1/2)M'_1} \delta_{\sigma+M_1, M'_1} \delta_{\sigma+M_2, M'_2}, \quad (29)$$

where the  $C_{j_1 m_1 j_2 m_2}^{j M}$  are the Clebsch–Gordan coefficients [50]. The expression (28) allows us to represent the total current as

$$I_{\text{tot}} = e \sum_{\sigma} g_{1\sigma} = e g_1^0 \eta(h). \quad (30)$$

The quantity  $g_1^0$  is defined by Eq. (11) with the low-temperature expression for the factor  $\Phi_v$ , Eq. (21), and with the parameter  $\alpha_0$ , Eq. (13), where  $V_{s-s} = V_{s-s}^0$ . In the low-temperature limit under consideration the main temperature dependence of the current together with the dependence on magnetic field is given by the factor

$$\eta(h) = \sum_{\sigma} \sum_{M_1, M'_1} \sum_{M_2, M'_2} W(M'_1, M'_2) \times |F(\sigma; M_1, M_2; M'_1, M'_2)|^2. \quad (31)$$

The quantity  $W(M'_1, M'_2)$  defines the weight of the spin states of a pair of paramagnetic ions for the case that the transferred electron is captured by

the first ion. We restrict ourselves to the case of fast spin-relaxation within each ion and obtain

$$W(M'_1, M_2) = Z^{-1} \exp[-E_{\text{mag}}(M'_1, M_2)/k_B T],$$

$$Z = \sum_{M'_1=-(S-1/2)}^{S-1/2} \sum_{M_2=-S}^S \exp[-E_{\text{mag}}(M'_1, M_2)/k_B T], \quad (32)$$

where  $E_{\text{mag}}(M'_1, M_2)$  is the magnetic energy of the ions. Providing that the frozen angular momentum of the ion is in its ground state, we can omit the spin-orbit interaction in the ground state. This interaction becomes important, however, when an extra electron is captured by the ion. In the simplest case, the spin-orbit interaction leads to a modification of  $g$ -factor as well as to an appearance of a single-ion anisotropy [51]. Below we consider the case of a weak alteration of the  $g$ -factor but take into consideration the contribution caused by the single-ion anisotropy. This allows us to represent the magnetic energy in the form, see also [18],

$$E_{\text{mag}}(M'_1, M_2) = \mu_B g [h_1 M'_1 + \text{sign}(h_2) h_2 M_2] + K(M'_1)^2, \quad (33)$$

where  $K > 0$  is the anisotropy constant, and  $h_1$  and  $h_2$  are the magnetic field-strengths acting on the separate paramagnetic ions.

Fig. 5 shows a steplike  $I(V)$ -characteristics depending on the direction of the magnetic fields. The appearance of plateaus can be explained in the following manner. At low temperatures as considered, only a small part of  $E_{\text{mag}}(M'_1, M_2)$  gives the main contribution to the current. If  $K = 0$  the corresponding energy is  $E_{\text{mag}}(M'_1 = -(S-1/2), M_2 = -S)$  ( $\mathbf{h}_1 \uparrow \uparrow \mathbf{h}_2$ ) or  $E_{\text{mag}}(M'_1 = -(S-1/2), M_2 = S)$  ( $\mathbf{h}_1 \uparrow \downarrow \mathbf{h}_2$ ). Thus, the projections  $M'_1 = -(S-1/2)$  for the first and  $M_2 = -S(S)$  for the second ion define the predominant ET channels. If a single-ion anisotropy is added (with  $K > 0$ ) it gives rise to a magnetic energy as soon as the absolute value of the  $M'_1$ th projection increases. Hence, each plateau reflects the competition between the Zeeman energy and the energy of the single-ion anisotropy. The magnetic field-strength  $h_{\text{switch}}$  at which the plateau with a particular projection  $M'_1$  merges to the plateau with the projection  $M'_1 - 1$  can be derived from

the condition  $E_{\text{mag}}(M'_1, M_2 = \pm S) = E_{\text{mag}}(M'_1 - 1, M_2 = \pm S)$  (the signs “+” and “-” indicate the cases  $\mathbf{h}_1 \uparrow \uparrow \mathbf{h}_2$  and  $\mathbf{h}_1 \uparrow \downarrow \mathbf{h}_2$ , respectively). This yields

$$h_{\text{switch}} = K(1 - 2M'_1)/\mu_B g. \quad (34)$$

This switching field does not depend on the projection of the second ion since its magnetic energy consists of only the Zeeman energy. It follows from condition  $h_{\text{switch}} > 0$  that each plateau is characterized by a definite spin-projection  $M'_1$  from the possible region

$$-1/2 \geq M'_1 \geq -(S-1/2). \quad (35)$$

This inequality allows us to determine the number of plateaus which exactly corresponds to the number of negative projections of the  $M'_1$ . If we chose  $S = 5/2$  ( $\text{Mn}^{2+}$  and  $\text{Fe}^{3+}$  paramagnetic ions) we can only observe two plateaus corresponding to the ET channels with  $M'_1 = -1, M_2 = -5/2$  and  $M'_1 = -2, M_2 = -5/2$  ( $\mathbf{h}_1 \uparrow \uparrow \mathbf{h}_2$ ), or alternatively to ET channels with  $M'_1 = -1, M_2 = +5/2$  and  $M'_1 = -2, M_2 = +5/2$  ( $\mathbf{h}_1 \uparrow \downarrow \mathbf{h}_2$ ). With increasing temperature, there exists no channel which assumes an appreciable weight to the current different from others; thus the plateaus become smeared out, cf. the dashed lines in Fig. 5.

To understand the strong decrease of the current if the direction of  $\mathbf{h}_2$  is changed we refer to the analysis of the saturated currents (last plateaus),  $M'_1 = -2, M_2 = -5/2$  ( $\mathbf{h}_1 \uparrow \uparrow \mathbf{h}_2$ ) and  $M'_1 = -2, M_2 = +5/2$  ( $\mathbf{h}_1 \uparrow \downarrow \mathbf{h}_2$ ). A detailed inspection of the corresponding Clebsch–Gordon coefficients shows that spin-dependent factor in Eq. (30) simplifies to

$$\eta(h) = \frac{(2S)^2}{(2S+1)^2}, \quad (\mathbf{h}_1 \uparrow \uparrow \mathbf{h}_2),$$

$$\eta(h) = \frac{2S}{(2S+1)^2}, \quad (\mathbf{h}_1 \uparrow \downarrow \mathbf{h}_2), \quad (36)$$

and thus the ratio of the saturated currents is equal to  $2S$ . The small current at  $\mathbf{h}_1 \uparrow \downarrow \mathbf{h}_2$  compared to  $\mathbf{h}_1 \uparrow \uparrow \mathbf{h}_2$  can be explained by the fact that the probability to transfer an electron between the ions with parallel spins is somewhat larger than for the transfer between the ions having an opposite spin direction. This behavior is reflected in the different form of the corresponding Clebsch–Gordon coefficients.

## 5. Conclusions

The focus of the present contribution has been on a detailed study of the  $I(V)$  and  $I(h)$  characteristics, respectively, of a *short molecular wire* and for the case where incoherent ET-transfer is responsible for the interelectrode current. The factors which substantially control the current are the polarization effect of the electrodes and the Coulomb repulsion between different transferred electrons. The image forces decrease the LUMO-levels of the wire units and in this manner reduce the gap between the levels of the terminal wire unit and the electrode Fermi-level up to some tenths of eV. For example, in the case of a wire with two units as depicted in Fig. 4 the gap of the isolated wire  $\Delta E_0 = 0.76$  eV is reduced to  $\Delta E = \Delta E_0 + E^{(i)}(x_1) = 0.27$  eV. Just this gap determines the voltage  $V = V_{\text{peak}}$  at which the maximal (peak) current is reached.

Moreover, the influence of the Coulomb repulsion between different transferred electrons has been statistically accounted for via the *transmission factor*  $W_0$ . It vanishes if only a single wire unit is completely occupied by the transferred electron because such a state is unable to conduct a further excess electron – until the first electron leaves the wire. Just the decreasing part of the (nonlinear) current as shown in Figs. 3 and 4 is originated by  $W_0$ . The concrete run of the  $I(V)$  curve follows from the competition between all single-electron transfer rates, see Fig. 1(a).

In Fig. 4 we showed the important case of a current which has a rather narrow peak in the vicinity  $V = V_{\text{peak}} \approx 1.9$  eV. A similar behavior has been observed in the experiments on a molecule which contains a nitroamine redox center [40]. The given explanation for the observed  $I(V)$ -characteristics are based on quantum-chemical calculations on the electronic energy level structure of the neutral molecule as well as for the presence of a single and two excess electrons in the molecule [42]. According to the obtained decrease of the LUMO-levels related to the presence of a single excess electron a second one should preferably enter the molecule. However, there is a serious problem within such an explanation, because no mechanism which may compensate the Coulomb

repulsion between the two excess electrons has been accounted for. In condensed media, however, such a mechanism results from a polarization of the surrounding medium. In the case of ET through a single molecule in a nanopore system, for example, one has to take into consideration not only the polarization of the nanopore itself but of the electrodes as well.

In our approach, the polarization effects substantially reduce the gap between the LUMO-level energies and the Fermi-energy, while the strong Coulomb repulsion blocks the simultaneous presence of two transferred electrons in the wire. This very blocking effect is responsible for the sudden decrease of the current and thus for its peak behavior. Let us estimate a peak value of the current represented in Fig. 4 where  $I_{\text{peak}} = 1.5 \times 10^{-7} I_s$  and  $I_s = e\chi_0$  with  $\chi_0$  given by Eq. (13). To estimate  $\chi_0$  we take  $E_F = 5$  eV. The coupling  $V_{s-e}$  between the terminal unit and the surface atom may strongly vary in dependency on the distance  $\delta$  as well as on structural and energetic characteristics of the unit and the surface. For example, the estimations carried out in the Newns–Anderson model indicate [52] that in the case of a *p*-benzene-dithiol wire  $V_{s-e} \approx 0.25$  eV. For our rough estimations we take  $V_{s-e} \approx (0.1–0.5)$  eV. It yields  $\chi_0 \sim (10^{13}–10^{14})$  s<sup>-1</sup>, and thus  $I_{\text{peak}} \sim (0.1–1)$  pA per a single wire. To compare this value with experimental results we take the data of [40]. The measured peak current through a certain area (nanopore) is found to be  $I_{\text{exp}}^{(\text{area})} = 1.03$  nA, while the common current density is around 53 A/cm<sup>2</sup>. Therefore, the area may be estimated as  $\sim 0.2 \times 10^{-10}$  cm<sup>2</sup>. Let the contact area which is related to a single conducting molecule amount  $(20–30)$  Å<sup>2</sup>, then the observed current  $I_{\text{exp}}^{(\text{area})} = 1.03$  nA is caused by  $\sim (10^3–10^4)$  molecules, i.e., an experimental peak current through a single molecule occurs at about  $(0.1–1)$  pA. This very value for  $I_{\text{peak}}$  is consistently predicted by our theory.

For the case of the magnetic field influence on the low-temperature current our discussion has concentrated only on the  $I(h)$ -characteristics. More extended calculations will be carried out if data on respective low-temperature experiments become available.

## Acknowledgements

The work was supported in part by the Russian–Ukrainian Programme on Nanophysics and Nanoelectronics (E.P.) and the Deutsche Forschungsgemeinschaft through Sonderforschungsbereich 486, project A 10 (P.H., E.P.).

## References

- [1] A. Aviram, M. Ratner, *Chem. Phys. Lett.* 29 (1974) 277.
- [2] F.L. Carter (Ed.), *Molecular Electronic Devices*, Marcel Dekker, New York, 1982.
- [3] A. Aviram (Ed.), *Molecular Electronics: Science and Technology*, AIP, New York, 1992.
- [4] M.C. Petty, M.R. Bryce, D. Bloor (Eds.), *An Introduction to Molecular Electronics*, Oxford University Press, New York, 1995.
- [5] G. Mahler, V. May, M. Schreiber (Eds.), *Molecular Electronics: Properties, Dynamics, and Applications*, Marcel Dekker, New York, 1996.
- [6] J. Jortner, M. Ratner (Eds.), *Molecular Electronics*, Blackwell Science, Oxford, UK, 1997.
- [7] A. Aviram, M. Ratner (Eds.), *Molecular Electronics: Science and Technology*, New York Academy of Sciences, New York, 1998.
- [8] R.M. Metzger, B. Chen, U. Höpfner, M.V. Lakshmikantham, D. Vuillaume, T. Kawai, X. Wu, H. Tashibana, T.V. Hughes, H. Sakurai, J.W. Baldwin, C. Hosch, M.P. Cava, L. Brehmer, G.J. Ashwell, *J. Am. Chem. Soc.* 119 (1997) 10455.
- [9] V. Mujica, A. Nitzan, Y. Mao, W. Davis, M. Kemp, A. Roitberg, M.A. Ratner, in: J. Jortner, M. Bixon (Eds.), *Electron Transfer: From Isolated Molecules to Biomolecules, Part II*, in: I. Prigogine, in: S.A. Rice (Eds.), *Adv. Chem. Phys. Ser.*, vol. 107, 1999, p. 403.
- [10] M. Reed, *Proc. IEEE* 87 (1999) 652.
- [11] V. Mujica, M. Kemp, M. Ratner, *J. Chem. Phys.* 101 (1994) 6849 (see also p. 6856).
- [12] V. Mujica, M. Kemp, A. Roitberg, M. Ratner, *J. Chem. Phys.* 104 (1996) 7296.
- [13] M. Magoga, C. Joachim, *Phys. Rev. B* 56 (1997) 4722.
- [14] M. Kemp, A. Roitberg, V. Mujica, T. Wanta, M.A. Ratner, *J. Phys. Chem.* 100 (1996) 8349.
- [15] S.N. Yaliraki, M.A. Ratner, *J. Chem. Phys.* 109 (1998) 5036.
- [16] E.G. Petrov, I.S. Tolokh, A.A. Demidenko, V.V. Gorbach, *Chem. Phys.* 193 (1995) 237.
- [17] E.G. Petrov, I.S. Tolokh, V. May, *Phys. Rev. Lett.* 79 (1997) 4006.
- [18] E.G. Petrov, I.S. Tolokh, V. May, *J. Chem. Phys.* 109 (1998) 9561.
- [19] H. Ness, A.J. Fisher, *Phys. Rev. Lett.* 83 (1999) 452.
- [20] A. Nitzan, *J. Phys. Chem. A* 105 (2001) 2677.
- [21] D. Segal, A. Nitzan, W.B. Dewis, M.R. Wasielewski, M. Ratner, *J. Phys. Chem. B* 104 (2000) 3817.
- [22] A. Nitzan, *Annu. Rev. Phys. Chem.* 52 (2001) 681.
- [23] E.G. Petrov, P. Hänggi, *Phys. Rev. Lett.* 86 (2001) 2862.
- [24] E.G. Petrov, Ya.R. Zelinskii, P. Hänggi, *Mol. Cryst. Liq. Cryst.* 361 (2001) 209.
- [25] M. Bixon, S. Jortner, *J. Phys. Chem. B* 104 (2000) 3096.
- [26] Y.A. Berlin, A.L. Burin, M. Ratner, *J. Am. Chem. Soc.* 123 (2001) 260.
- [27] E.G. Petrov, Y.e.V. Shevchenko, V.I. Teslenko, V. May, *J. Chem. Phys.* 115 (2001) 7107.
- [28] V. May, *J. Mol. Electron.* 6 (1990) 187.
- [29] V. May, *Phys. Lett. A* 161 (1991) 118.
- [30] G. Treboux, *J. Phys. Chem. B* 104 (2000) 9823.
- [31] V. Mujica, A.E. Roitberg, M. Ratner, *J. Chem. Phys.* 112 (2000) 6834.
- [32] S. Jorgensen, M. Ratner, K.V. Mikkelsen, *J. Chem. Phys.* 114 (2001) 3790 (see also p. 3800).
- [33] W. Tian, S. Datta, S. Hong, R. Reifenberger, J.I. Henderson, C.P. Kubiak, *J. Chem. Phys.* 109 (1998) 2874.
- [34] S.N. Yaliraki, A.E. Roitberg, C. Gonzales, V. Mujica, M.A. Ratner, *J. Chem. Phys.* 111 (1999) 6997.
- [35] S.N. Yaliraki, M. Kemp, M.A. Ratner, *J. Am. Chem. Soc.* 121 (1999) 3428.
- [36] Y. Xue, S. Datta, M.A. Ratner, *J. Chem. Phys.* 115 (2001) 4292.
- [37] C. Joachim, J.P. Launay, *J. Mol. Electron.* 6 (1990) 37.
- [38] J.M. Tour, *Chem. Rev.* 96 (1996) 537; J.M. Tour, M. Kozaki, J.M. Seminario, *J. Am. Chem. Phys.* 120 (1998) 8486.
- [39] D.L. Klein, P.L. Euen, J.E.B. Katari, R. Roth, A.P. Alivisatos, *Appl. Phys. Lett.* 68 (1995) 2574; C. Boulas, J.V. Davidovits, E. Rondelez, D. Vijillaume, *Phys. Rev. Lett.* 76 (1996) 4797; L.A. Bumm, J.J. Arnold, M.T. Cygan, T.D. Dunbar, T.P. Burgin, L. Jones II, D.L. Allara, J.M. Tour, P.S. Weiss, *Science* 271 (1996) 1705; A. Dhirani, P.-H. Lin, P. Gayot-Sionnest, R.W. Zehner, L.R. Sita, *J. Chem. Phys.* 106 (1997) 5249; S. Datta, W. Tian, S. Hong, R. Reifenberger, C.P. Kubiak, *Phys. Rev. Lett.* 79 (1997) 2530.
- [40] J. Chen, M.A. Reed, A.M. Rawlett, J.M. Tour, *Science* 286 (1999) 550.
- [41] J.M. Seminario, A.G. Zacarias, J.M. Tour, *J. Phys. Chem. A* 103 (1999) 7883; J. Chen, W. Wang, M.A. Reed, A.M. Rawlett, D.W. Price, J.M. Tour, *Appl. Phys. Lett.* 77 (2000) 1224; F. Moresco, G. Meyer, K.-H. Rieder, *Phys. Rev. Lett.* 86 (2001) 672.
- [42] J. Seminario, A.G. Zacarias, J.M. Tour, *J. Am. Chem. Soc.* 122 (2000) 3015.
- [43] S.A. Gurvitz, H.J. Lipkin, Ya.S. Prager, *Phys. Lett. A* 212 (1996) 91.
- [44] J. Jortner, *J. Chem. Phys.* 64 (1976) 4860.
- [45] L.D. Landau, L.M. Lifshitz, *Electrodynamics of Continuous Media*, Pergamon Press, Oxford, 1975.

- [46] I.S. Gradshtein, I.M. Ryzhik, *Tables of Integrals, Series, and Products*, fifth ed., Academic Press, San Diego, 1994.
- [47] J.J. Markham, *Rev. Mod. Phys.* 31 (1959) 956.
- [48] R.L. Carlin, *Magnetochemistry*, Springer, Berlin, 1986.
- [49] E.G. Petrov, I.S. Tolokh, V. May, *J. Chem. Phys.* 108 (1998) 4386.
- [50] A.S. Davydov, *Quantum Mechanics*, second ed., Pergamon Press, Oxford, 1976.
- [51] A. Abraham, B. Bleaney, *Electron Paramagnetic Resonance of Transition Ions*, Clarendon, Oxford, 1970.
- [52] M. Olson, Y. Mao, T. Windus, M. Kemp, M. Ratner, *J. Phys. Chem. B* 102 (1998) 941.